CD40 induces macrophage anti–*Toxoplasma gondii* activity by triggering autophagy-dependent fusion of pathogen-containing vacuoles and lysosomes

Rosa M. Andrade,[1] Matthew Wessendarp,[1] Marc-Jan Gubbels,[2] Boris Striepen,[2] and Carlos S. Subauste[1]

[1]Division of Infectious Diseases, Department of Internal Medicine, University of Cincinnati College of Medicine, Cincinnati, Ohio, USA.
[2]Center for Tropical and Emerging Global Diseases, University of Georgia, Athens, Georgia, USA.

Many intracellular pathogens, including *Toxoplasma gondii*, survive within macrophages by residing in vacuoles that avoid fusion with lysosomes. It is important to determine whether cell-mediated immunity can trigger macrophage antimicrobial activity by rerouting these vacuoles to lysosomes. We report that CD40 stimulation of human and mouse macrophages infected with *T. gondii* resulted in fusion of parasitophorous vacuoles and late endosomes/lysosomes. Vacuole/lysosome fusion took place even when CD40 was ligated after the formation of parasitophorous vacuoles. Genetic and pharmacological approaches that impaired phosphoinositide-3-class 3 (PIK3C3), Rab7, vacuolar ATPase, and lysosomal enzymes revealed that vacuole/lysosome fusion mediated antimicrobial activity induced by CD40. Ligation of CD40 caused colocalization of parasitophorous vacuoles and LC3, a marker of autophagy, which is a process that controls lysosomal degradation. Vacuole/lysosome fusion and antimicrobial activity were shown to be dependent on autophagy. Thus, cell-mediated immunity through CD40 stimulation can reroute an intracellular pathogen to the lysosomal compartment, resulting in macrophage antimicrobial activity.

Introduction

Macrophages are pivotal effectors for control of intracellular pathogens. Fusion of the lysosomal compartment with vacuoles that contain these pathogens is a fundamental mechanism by which macrophages kill microbes. Unfortunately, many pathogens manipulate vesicular trafficking and, as a result, avoid fusion with lysosomes, allowing their survival within macrophages (1–3). Thus, it is crucial to determine whether cell-mediated immunity (CMI) can activate phagolysosomal fusion for control of intracellular pathogens. *Toxoplasma gondii*, a major pathogen in patients with defects in CMI, provides an excellent model for addressing this question. While a recent study revealed that this obligate intracellular protozoan hijacks mammalian lysosomes in the vacuolar space (4), no actual fusion of the parasitophorous vacuole (PV) with the lysosomal compartment takes place, enabling *T. gondii* to survive within host cells (4–6). The fate of *T. gondii* within host cells is thought to be determined at the time of cell entry; active invasion results in a nonfusogenic PV, allowing parasite replication, while uptake through Fc receptors leads to phagolysosomal fusion and killing of the pathogen (5, 6).

The fact that many pathogens cannot survive within lysosomes raises the possibility that targeting them to this compartment would result in pathogen eradication. There is controversy as to whether TLRs modulate phagolysosomal fusion. While one study reported that TLR signaling accelerates the rate of this process (7), another group found that neither TLR2 nor TLR4 control the rate of phagosome acidification or phagolysosome fusion (8). An association between IFN-γ and phagolysosomal fusion has been observed (9, 10). However, using *T. gondii* as a model, a recent study showed that IFN-γ induces antimicrobial activity independently of phagosomal maturation (11). Taken together, it is not certain whether CMI utilizes fusion of pathogen-containing vacuoles and lysosomes as a mechanism to control intracellular pathogens.

Lysosomal degradation as a mechanism to kill pathogens that normally reside within nonfusogenic vacuoles would require rerouting these vacuoles to the lysosomal compartment. In this regard, autophagy is a process that directs cytoplasmic material and organelles to the lysosomes (12, 13). In this process, portions of cytosol and organelles are encircled by autophagosomes. This is followed by fusion between autophagosomes and endosomes/lysosomes, culminating in the formation of autolysosomes and degradation of their contents (14). Thus, autophagy represents an alternate route to the lysosomal compartment. Under certain conditions, host cells can degrade *Shigella flexneri* and *Streptococcus pyogenes* through autophagy (15, 16). While *S. flexneri* within epithelial cells normally avoids the autophagic pathway, experimental deletion of the bacterial gene *icsB* results in bacterial death via autophagy (16). Epithelial cells invaded by *S. pyogenes* and treated with antibiotics exhibit a transient

Nonstandard abbreviations used: CMI, cell-mediated immunity; CPSII, carbamoyl phosphate synthetase II; EGFP, enhanced GFP; hCD154, human CD154; hmCD40, chimera of the extracellular domain of human CD40 and the intracytoplasmic domain of mouse CD40; LAMP-1, lysosome-associated membrane glycoprotein 1; LC3, light chain 3; 3-MA, 3-methyladenine; M6PR, mannose 6-phosphate receptor; ODN, oligodeoxynucleotide; PIK3C3, phosphoinositide-3-kinase class 3; PV, parasitophorous vacuole; RNI, reactive nitrogen intermediate; SAG1, surface antigen 1; secRFP, secreted red fluorescent protein; YFP, yellow fluorescent protein.

Conflict of interest: The authors have declared that no conflict of interest exists.

Citation for this article: *J. Clin. Invest.* **116**:2366–2377 (2006). doi:10.1172/JCI28796.

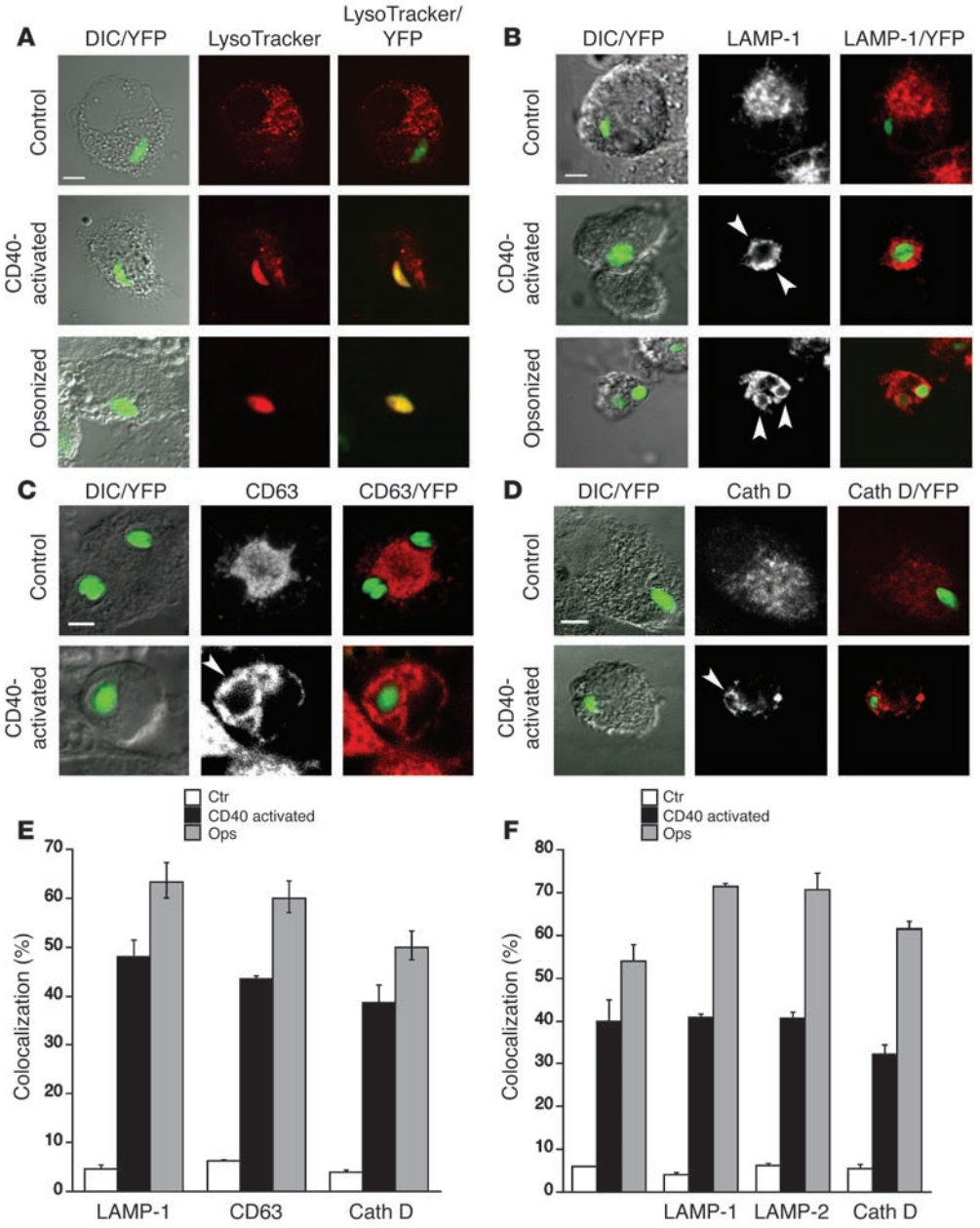

Figure 1

CD40 stimulation induces vacuole/lysosome fusion in human and mouse macrophages infected with *T. gondii*. (**A**) Control and CD154-stimulated human macrophages were incubated with LysoTracker Red, then infected with *T. gondii*–YFP. Macrophages incubated with opsonized *T. gondii* were used as controls. Cells were examined by confocal microscopy 6 hours after infection or 2 hours after addition of opsonized parasites. Macrophages shown contain 1 tachyzoite of *T. gondii*. (**B**–**D**) Control and CD40-activated human macrophages were infected with *T. gondii*–YFP. Macrophages incubated with opsonized *T. gondii* were used as controls. Macrophages were incubated with anti–LAMP-1 (**B**), anti-CD63 (**C**), or anti-cathepsin D (**D**) Abs; this was followed by addition of secondary antibodies. Cells were examined by confocal microscopy at 6 hours after infection or 1 hour after addition of opsonized *T. gondii*. CD40-activated macrophages show colocalization of LAMP-1, CD63, and cathepsin D (rings) around *T. gondii*–containing vacuoles (arrowheads). Cath, cathepsin. Scale bars: 5 μm. (**E** and **F**) Quantification of colocalization of late endosomal/lysosomal markers around vacuoles containing *T. gondii* within human (**E**) or mouse (**F**) primary macrophages. Monolayers were examined at 6 and 8 hours after challenge in the case of human and mouse macrophages, respectively. In the case of macrophages incubated with opsonized *T. gondii,* M6PR was assessed at 15 minutes while LAMP-1, LAMP-2, CD63, and cathepsin D expression were assessed at 1 hour. Percentages indicate the mean ± SD. Results shown are representative of 3–4 independent experiments. Cath, cathepsin; ctr, control; DIC, differential interface contrast; ops, opsonized.

autophagy-dependent degradation of the bacteria (15). However, it is unclear whether autophagy is a mechanism used by CMI to eradicate pathogens. A recent study indicates that induction of autophagy in macrophages by starvation or rapamycin inhibits viability of *Mycobacterium tuberculosis* (17). Moreover, IFN-γ stimulates autophagy in macrophages, and this process is accompa-

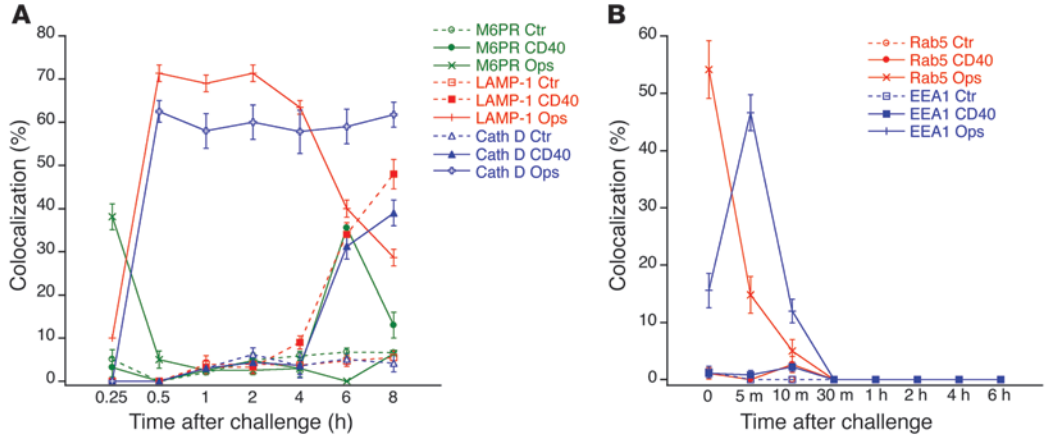

Figure 2
Kinetics of recruitment of endosomal and lysosomal markers. Mouse peritoneal macrophages were incubated with control (ctr) or anti-CD40 mAbs, then infected with *T. gondii*. Expression of late endosomal and lysosomal markers (**A**) or early endosomal markers (**B**) was examined by immunofluorescence at different times after challenge. Opsonized tachyzoites were used as positive control. Results are shown as the mean ± SD and are representative of 3 independent experiments.

nied by recruitment of autophagy markers to the mycobacterial phagosome (17). However, no demonstration was provided that IFN-γ acted through autophagy to induce macrophage antimicrobial activity. Moreover, studies in a model of *T. gondii* infection did not find evidence that IFN-γ induces antimicrobial activity through autophagy (11). Thus, the crucial question that remains to be answered is whether autophagy mediates pathogen eradication triggered by CMI. Such a demonstration would provide important new insights into host-pathogen interaction and mechanisms of host protection.

The interaction between CD40 and CD154 (expressed primarily on antigen-presenting cells and activated $CD4^+$ T cells, respectively) is an event during CMI that is central for host protection. Communication between T cells and macrophages through this pathway induces macrophage microbicidal activity against numerous pathogens, including *T. gondii* (18), an effect that likely contributes to in vivo resistance against these organisms (18–22). While reactive nitrogen intermediates (RNIs) can mediate macrophage antimicrobial activity induced by CD40, experimental evidence indicates the existence of other mechanisms of pathogen control. CD40 engagement directly activates macrophages to restrict the growth of *Mycobacterium avium* despite the fact that this pathogen is not controlled by RNI in activated macrophages (21). In the case of *T. gondii*, CD40 induces macrophage toxoplasmacidal activity that is independent not only of RNI but also of IFN-γ, STAT1, the p47 GTPases LRG-47, IGTP, and IRG-47, production of oxygen intermediates, or tryptophan starvation (23–25). Using *T. gondii* as a model, we examined whether CD40 engagement can alter the fate of *T. gondii* by inducing fusion between PV and the late endosomal/lysosomal compartments and whether such a response is mediated by autophagy. These studies have implications for understanding the biology of *T. gondii* infection in vivo since engagement of CD40 leads to IFN-γ–RNI-, STAT1-independent macrophage toxoplasmacidal activity and in vivo restriction of *T. gondii* growth (24).

Results

CD40 stimulation recruits late endosomal/lysosomal markers to vacuoles containing T. gondii. We tested to determine whether CD40 stimulation of macrophages induces fusion between *T. gondii*–containing vacuoles and late endosomes/lysosomes. Human monocyte–derived macrophages were infected with transgenic *T. gondii*, which expresses yellow fluorescent protein (YFP). CD40 stimulation does not affect the initial percentage of infected macrophages (25). Staining with an antibody against the parasite antigen surface antigen 1 (SAG1), then an Alexa 568–conjugated secondary antibody in nonpermeabilized monolayers revealed that the percentages of cell-associated *T. gondii* that resided within macrophages were similar in control and CD40-activated monolayers (control: 87.7% ± 2.4%; CD40 activated:

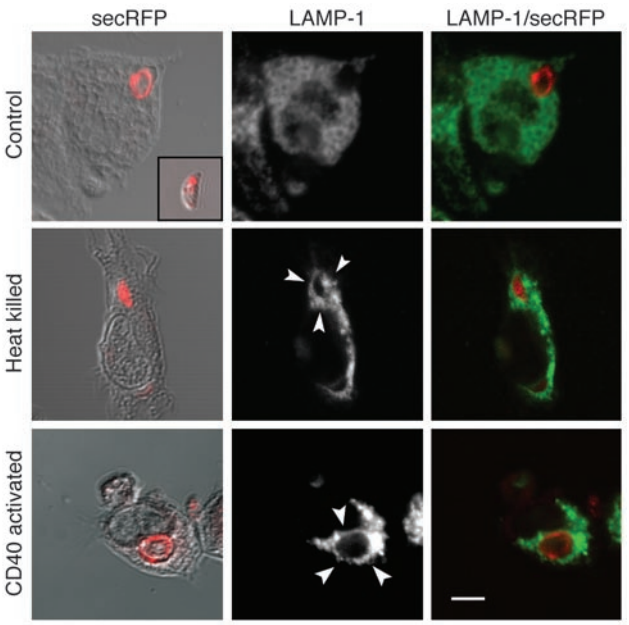

Figure 3
CD40 stimulation induces convergence of PV and late endosomes/lysosomes. Mouse resident peritoneal macrophages were incubated with control or stimulatory anti-CD40 mAbs, then challenged with *T. gondii*–secRFP. Expression of LAMP-1 was assessed at 8 hours after challenge. Inset represents an extracellular tachyzoite with accumulation of fluorescence in dense granules. Macrophages were also incubated with heat-killed *T. gondii*–secRFP, and LAMP-1 expression was assessed at 1 hour after challenge. Arrowheads indicate colocalization of LAMP-1 around *T. gondii*–containing compartments. Scale bar: 5 μm. Results are representative of 4 independent experiments.

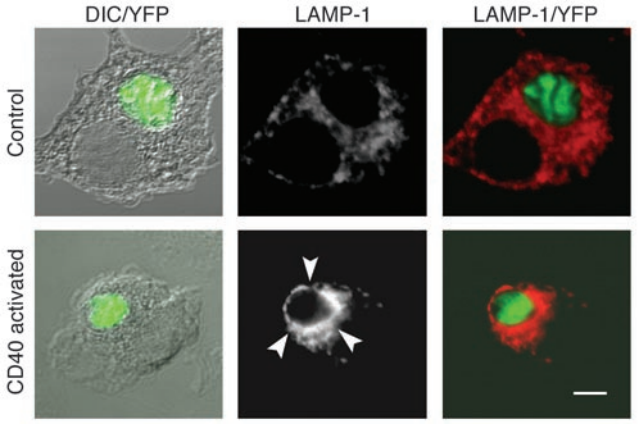

Figure 4
CD40 stimulation induces fusion of preformed PV and late endosomes/lysosomes. Bone marrow macrophages from TNF-$\alpha^{-/-}$ mice infected with CPSII KO *T. gondii*–YFP were incubated overnight in the presence of uracil (0.2 mM) to allow parasite replication. After uracil removal, infected macrophages were cultured with stimulatory anti-CD40 mAb for 24 hours. TNF-α (500 pg/ml) was then added to monolayers, and cells were examined after 7 hours. Arrowheads denote colocalization of LAMP-1 (ring) around PV in CD40-activated macrophage. Scale bar: 5 μm. Results are representative of 4 independent experiments.

85.5% ± 2.6%; $P = 0.4$; $n = 3$). Next, macrophages were loaded with the acidotropic dye LysoTracker Red, which labels late endosomes/lysosomes. Parasites in control macrophages resided in a compartment that largely excluded LysoTracker Red (colocalization: 4.9% ± 1.5%; $n = 4$) (Figure 1A). In contrast, uptake of opsonized *T. gondii*–YFP revealed accumulation of LysoTracker Red in parasite-containing phagosomes (colocalization: 60.6% ± 2.9%). Importantly, CD40-activated macrophages infected with nonopsonized *T. gondii*–YFP exhibited a significant increase in colocalization of LysoTracker Red and parasite-containing vacuoles compared with control macrophages (colocalization: 46.5% ± 3.6%; $P < 0.0001$) (Figure 1A).

We examined the expression of lysosome-associated membrane protein 1 (LAMP-1), CD63, and cathepsin D to confirm that CD40 stimulation results in fusion between *T. gondii*–containing vacuoles and late endosomes/lysosomes. Macrophages that phagocytosed opsonized *T. gondii* revealed a distinct rim of fluorescence around the phagosome, indicative of phagolysosomal fusion (5) (Figure 1B). Most control macrophages infected with *T. gondii* exhibited vacuoles that did not colocalize LAMP-1, CD63, and cathepsin D. In contrast, CD40 stimulation resulted in a significant increase (6.8- to 10.4-fold increase; $P < 0.0003$) in the percentage of macrophages that revealed colocalization of LAMP-1, CD63, and cathepsin D around the vacuoles (Figure 1, B–E). Colocalization with late endosomal/lysosomal markers was also observed in mouse macrophages (Figure 1F). CD40 stimulation of mouse peritoneal macrophages significantly increased (5.9- to 10.3-fold increase; $P < 0.0009$) localization of mannose 6-phosphate receptor (M6PR), LAMP-1, LAMP-2, and cathepsin D around *T. gondii*–containing vacuoles compared with control macrophages (Figure 1F). Not all macrophages express CD40 (23). Thus, we examined CD40 and LAMP-1 expression. Most (79.2% ± 4.2%; $P = 0.0007$) $CD40^+$ macrophages from the CD40-stimulated monolayers exhibited colocalization of LAMP-1 around the vacuoles (Supplemental Figure 1; supplemental material available online with this article; doi:10.1172/JCI28796DS1). In contrast, the percentage of macrophages with colocalization of LAMP-1 around the vacuoles remained unchanged in $CD40^+$ and $CD40^-$ macrophages from control monolayers and in $CD40^-$ macrophages from $CD40^-$–stimulated monolayers (8.3% to 13.0%; $P = 0.7$). Taken together, CD40 stimulation of human and mouse macrophages results in a pattern of localization of late endosomal/lysosomal markers compatible with fusion with *T. gondii*–containing vacuoles, an interpretation further supported by the distinct overlap between LysoTracker Red and these vacuoles.

Vacuole/lysosome fusion takes place in CD40-activated macrophages that were invaded by T. gondii tachyzoites. Compared with classical phagolysosomal fusion triggered by Fc receptor–mediated phagocytosis, vacuole/lysosome fusion induced by CD40 was

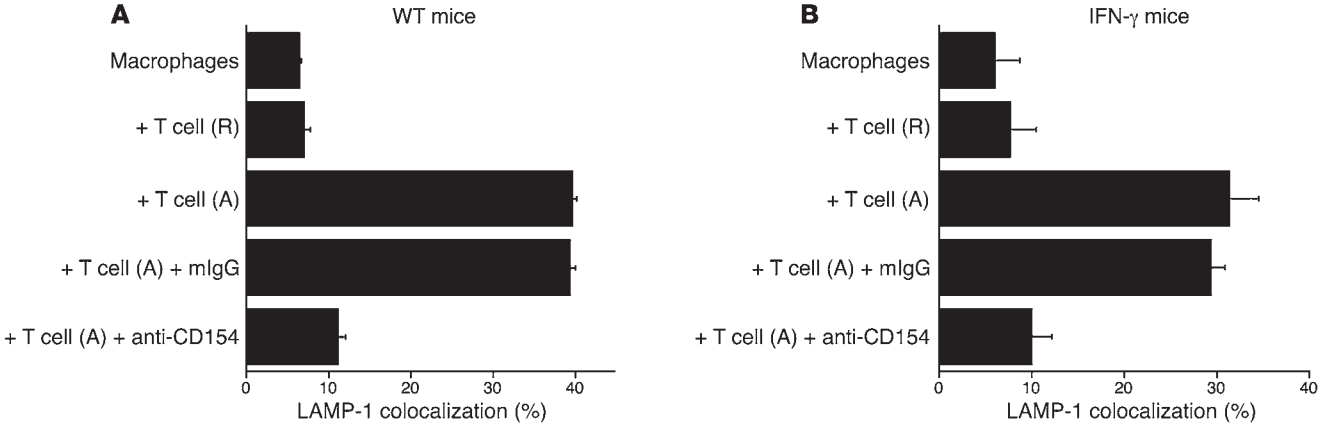

Figure 5
Activated $CD4^+$ T cells induce vacuole/lysosome fusion through CD40/CD154 interaction. Peritoneal macrophages from WT mice (**A**) or IFN-$\gamma^{-/-}$ mice (**B**) were infected with *T. gondii*–YFP and incubated for 10 minutes; this was followed by removal of extracellular parasites. After 1 hour, either resting (R) or activated (A) $CD4^+$ T cells from WT (**A**) or IFN-$\gamma^{-/-}$ (**B**) mice were added in the presence of anti-CD54 or control mAbs. Colocalization of LAMP-1 around PV was assessed by immunofluorescence 8 hours after infection. Results are shown as the mean ± SD and are representative of 4 independent experiments.

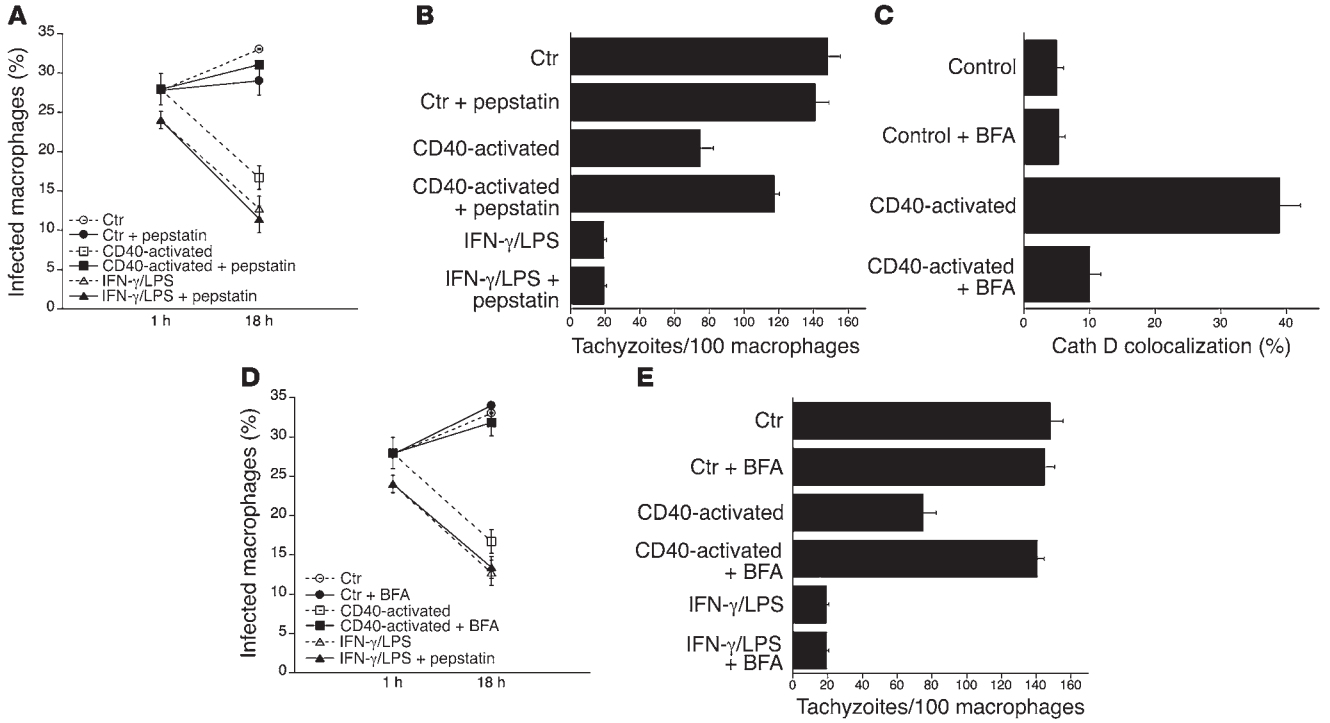

Figure 6
Vacuole/lysosome fusion mediates macrophage antimicrobial activity induced by CD40. Mouse peritoneal macrophages were incubated with control or anti-CD40 mAbs or with IFN-γ/LPS, then infected with *T. gondii*. (**A** and **B**) Pepstatin (50 μM) was added 1 hour after infection. Percentage of infected macrophages and parasite load was assessed by light microscopy at 1 and 18 hours after challenge. (**C**–**E**) Bafilomycin A (BFA; 25 nM) was added 1 hour before infection with *T. gondii*. (**C**) Expression of cathepsin D was examined by immunofluorescence 8 hours after infection. (**D**) Percentage of infected macrophages and parasite load were assessed at 1 and 18 hours after challenge. (**E**) Parasite load was determined at 18 hours. Results are shown as the mean ± SD and are representative of 4 independent experiments.

delayed and did not appear to be accompanied by recruitment of early endosomal markers (Figure 2). Interestingly, examination of CD40-activated macrophages 6 to 8 hours after infection revealed that 52.8% ± 3.0% of the vacuoles that colocalized with late endosomal/lysosomal markers already contained 2 tachyzoites (n = 6). These findings suggested that fusion took place with vacuoles that were formed by invasion of viable parasites. We conducted studies to further examine this possibility. Active invasion of host cells and formation of PVs is characterized by secretion of contents from the parasite-dense granules into the vacuoles (26). This process does not occur during phagocytosis of parasites. To confirm that tachyzoites resided in a PV, experiments were conducted with transgenic *T. gondii*, which express a fusion protein consisting of P30 major surface antigen and a secreted red fluorescent protein (DsRed; *T. gondii*–secRFP; the GPI anchor attachment signal was deleted to generate a soluble reporter). As reported (27), extracellular parasites exhibited cytoplasmic fluorescence that accumulated in dense granules (Figure 3). Infection of control macrophages by viable *T. gondii*–secRFP resulted in a shift in fluorescence from within the parasites to the vacuolar lumen surrounding the parasites (Figure 3). In contrast, phagocytosis of heat-killed tachyzoites did not result in a fluorescence shift (Figure 3). Next, we examined expression of LAMP-1 in control and CD40-activated macrophages infected with *T. gondii*–secRFP. No accumulation of LAMP-1 was noted around vacuoles with intraluminal red fluorescence in infected control macrophages. Importantly, 42.1% ± 2.4% of infected CD40-activated macrophages revealed colocalization of LAMP-1 around vacuoles with intraluminal red fluorescence. Thus, CD40 stimulation results in fusion between late endosomes/lysosomes and PVs formed by invasion of viable tachyzoites.

CD40 engagement induces vacuole/lysosome fusion in macrophages with previously formed PVs. We conducted additional experiments to further explore whether CD40 switches the fusogenic potential of PVs. Carbamoyl phosphate synthetase II (CPSII) KO *T. gondii* exhibit unimpaired capacity to infect host cells but require exogenous uracil for multiplication, and removal of this nucleotide arrests their replication (28). We used transgenic CPSII KO tachyzoites that express cytosolic YFP to determine whether CD40 stimulation induces fusion with preformed PVs. This experiment was based on our prior demonstration that CD40 triggers macrophage toxoplasmacidal activity by enhancing autocrine production of TNF-α followed by cooperation between CD40 and TNF-α (25, 29). Bone marrow–derived macrophages from TNF-$\alpha^{-/-}$ mice were infected with CPSII KO *T. gondii*–YFP and were cultured in the presence of uracil. Uracil was removed after overnight incubation, at which time vacuoles contained typically 4 parasites. Macrophages were then incubated with or without a stimulatory anti-CD40 mAb followed by addition of TNF-α. PV in control macrophages did not colocalize with LAMP-1 (Figure 4). In contrast, colocalization of LAMP-1 and preformed PVs was observed in 27.3% ± 1.8% of TNF-$\alpha^{-/-}$ macrophages

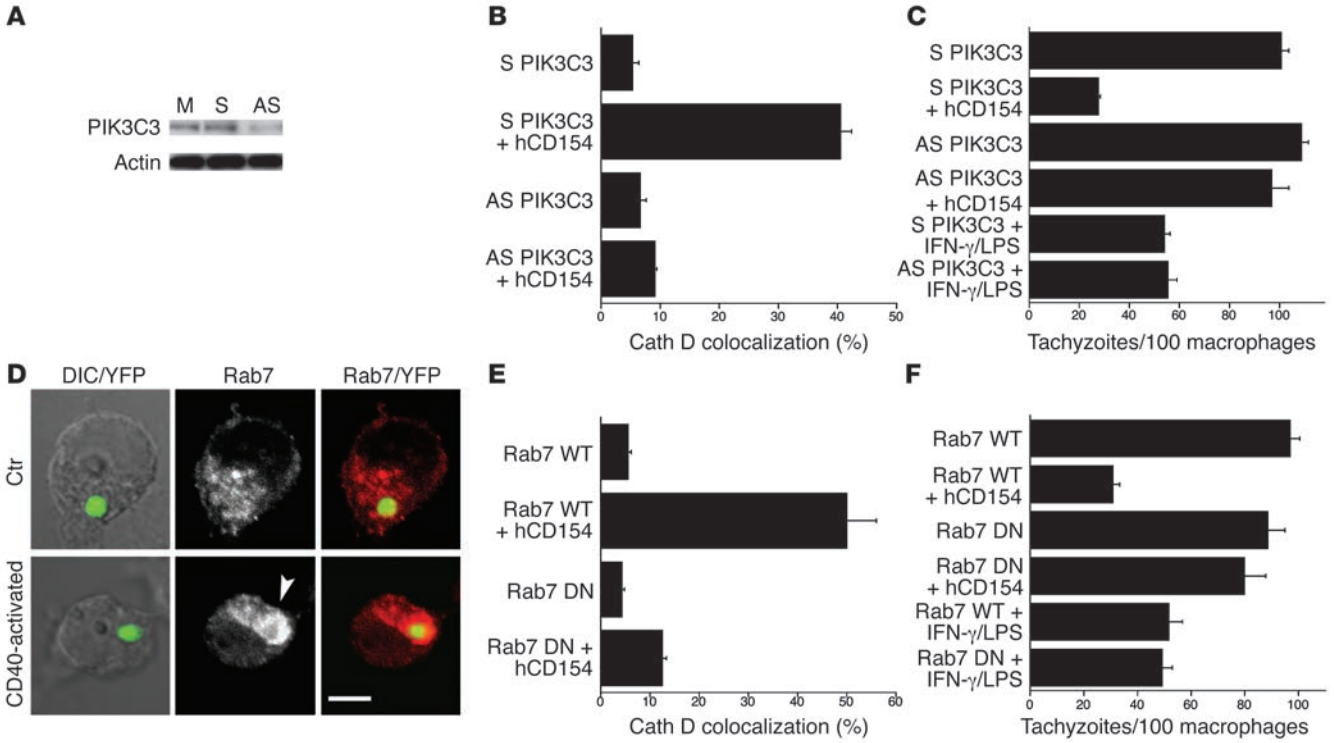

Figure 7

Blockade of vacuole/lysosome fusion ablates CD40-induced antimicrobial activity. The effects of knockdown of PIK3C3 (**A**–**C**) and Rab7 dominant-negative mutant (**D**–**F**) on vacuole/lysosome fusion and antimicrobial activity were examined. (**A**) hmCD40–RAW 264.7 cells were mock transfected (M) or were transfected with sense (S) or antisense (AS) ODN against PIK3C3. Protein expression of PIK3C3 and actin were analyzed 48 hours after transfection. (**B**) Transfected cells were incubated with or without hCD154, then infected with *T. gondii*–YFP. Vacuole/lysosomal fusion was assessed by cathepsin D staining 8 hours after infection. (**C**) Transfected cells were treated with medium alone, hCD154, or IFN-γ/LPS; this was followed by *T. gondii* infection. Cells were examined by light microscopy 18 hours after infection. (**D**) CD40-activated and control mouse peritoneal macrophages were infected with *T. gondii*–YFP followed by assessment of Rab7 expression by immunofluorescence. Arrowhead denotes colocalization of Rab7 (ring) around *T. gondii*–containing vacuole in CD40-activated macrophage. Scale bar: 5 μm. (**E**) hmCD40–RAW 264.7 cells were incubated with medium with or without hCD154 followed by transfection with Rab7 WT or Rab7(T22N). Cells were infected with *T. gondii*–RFP. Vacuole/lysosomal fusion was assessed by cathepsin D staining 8 hours after infection. (**F**) Transfected hmCD40–RAW 264.7 cells treated with medium alone, CD154, or IFN-γ/LPS were challenged with *T. gondii*. Cells were examined by light microscopy 18 hours after challenge. Results are shown as the mean ± SD and are representative of 4 independent experiments. DN, dominant negative.

stimulated through CD40 and incubated with TNF-α (Figure 4). These activated macrophages exhibited a 35.3% ± 3.2% reduction in the percentage of infected cells at 24 hours compared with control macrophages. Thus, CD40 stimulation induces vacuole/lysosome fusion in preformed PVs.

CD154$^+$CD4$^+$ T cells induce vacuole/lysosome fusion in macrophages previously infected with viable T. gondii in an IFN-γ–independent manner. CD154 exists in a membrane-bound and a soluble form. Membrane CD154 is expressed primarily on activated CD4$^+$ T cells, suggesting a scenario in which membrane CD154 would engage CD40 on macrophages previously infected with an intracellular pathogen. Activated CD4$^+$ T cells induce CD154-dependent anti–*T. gondii* activity in macrophages (23). Thus, we determined whether activated CD4$^+$ T cells trigger vacuole/lysosome fusion in macrophages previously infected with *T. gondii*. Mouse peritoneal macrophages were infected with *T. gondii*–YFP or *T. gondii*–secRFP. Resting or activated CD4$^+$ T cells were added after 1 hour. Activated but not resting CD4$^+$ T cells caused colocalization of LAMP-1 around *T. gondii*–containing vacuoles (Figure 5A). Fusion with late endosomes/lysosomes was inhibited by a mAb against CD154 (81.8% ± 2.8% inhibition; $P = 0.0001$). Vacuole/lysosome fusion did not require IFN-γ because similar results were obtained with activated CD4$^+$ T cells and macrophages from IFN-γ$^{-/-}$ mice (Figure 5B). Thus, CD40-CD154 interaction during the crosstalk between T cells and macrophages induces vacuole/lysosome fusion independently of IFN-γ.

Vacuole/lysosome fusion mediates anti–T. gondii activity induced by CD40 stimulation. We took several approaches to determine if vacuole/lysosome fusion mediates toxoplasmacidal activity induced by CD40. First, we examined the effects of inhibitors of hydrolytic enzymes on anti–*T. gondii* activity induced by CD40 stimulation. Control and CD40-activated primary mouse macrophages were infected with *T. gondii* followed by addition of pepstatin, an inhibitor of cathepsin D. Not all primary macrophages express CD40, and only CD40$^+$ macrophages acquire toxoplasmacidal activity in response to CD40 ligation (23, 25). Indeed, primary macrophages incubated with a stimulatory anti-CD40 mAb exhibited on average a 55.3% ± 1.9% decrease in parasite load. Pepstatin did not affect the percentage of infection and parasite load in control macrophages (Figure 6, A and B). In

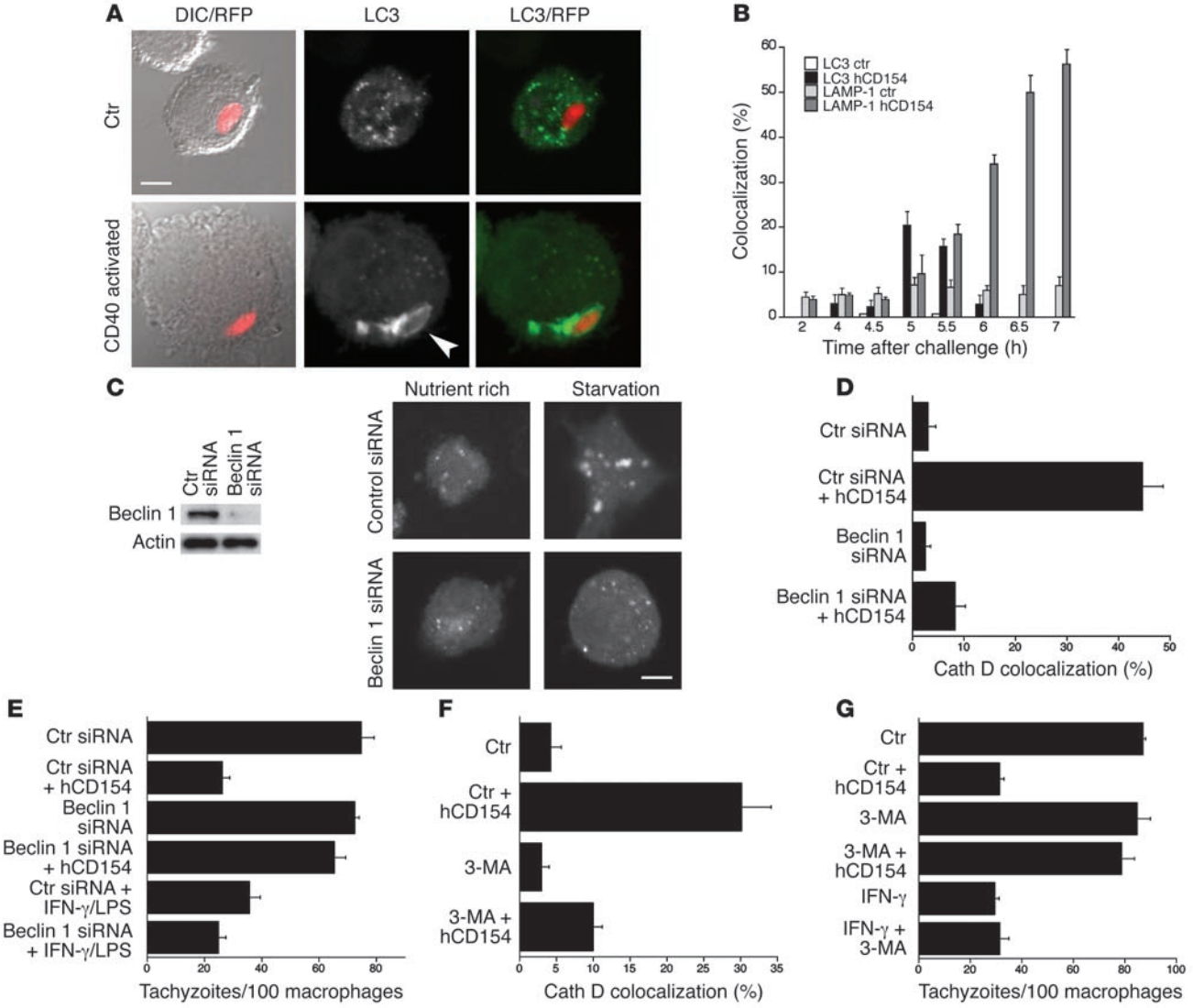

Figure 8

CD40 stimulation induces vacuole/lysosome fusion and antimicrobial activity through autophagy. (**A**) Control and CD40-activated hmCD40–RAW 264.7 cells were transfected with LC3-EGFP and infected with *T. gondii*–RFP. Monolayers were examined by confocal microscopy at 5 hours after challenge. Arrowhead indicates accumulation of LC3 around vacuole. Scale bars: 5 μm. (**B**) Kinetics of colocalization of LC3 and LAMP-1 around PV in hmCD40–RAW 264.7 cells. (**C**) hmCD40–RAW 264.7 cells were transfected with control or Beclin 1 siRNA. Immunoblot was performed after 96 hours. Two days after transfection with control or Beclin 1 siRNA, hmCD40–RAW 264.7 cells were transfected with LC3-EGFP, then incubated in complete medium or HBSS for 1 hour. Expression of LC3 was analyzed by confocal microscopy. (**D**) Control or CD40-activated hmCD40–RAW 264.7 cells transfected with control or Beclin 1 siRNA were infected with *T. gondii*–YFP, then stained for cathepsin D 8 hours after infection. Percentages of vacuoles that colocalized with cathepsin D were assessed by immunofluorescence. (**E**) Control, CD40-activated, or IFN-γ/LPS–treated hmCD40–RAW 264.7 cells transfected with control or Beclin 1 siRNA were infected with *T. gondii* followed by assessment of parasite load by light microscopy 18 hours after infection. (**F** and **G**) Control, CD40-, or IFN-γ–activated human monocyte–derived macrophages were infected with *T. gondii*, then incubated with or without 3-MA (10 mM). Expression of cathepsin D was examined by immunofluorescence 6 hours after infection (**F**), and parasite load was assessed at 18 hours after infection (**G**). Results are shown as the mean ± SD and are representative of 3 to 4 independent experiments.

contrast, pepstatin remarkably inhibited the drop in infection rate induced by CD40 stimulation and the reduction in parasite load in these macrophages (81.8% ± 4.3% inhibition; $P < 0.01$). In parallel studies, pepstatin did not affect anti–*T. gondii* activity induced by IFN-γ/LPS. Similar results were obtained with leupeptin, an inhibitor of serine and cysteine proteases (Supplemental Figure 2, A and B).

Vacuolar ATPase and phosphoinositide-3-kinase class 3 (PIK3C3), also known as hVps34, are required for transport to late endosomes and lysosomes (30, 31). Indeed, bafilomycin A, a specific inhibitor of vacuolar ATPase, reduces delivery of endosomal cargo to lysosomes and mixing of phagosome and lysosome contents while LY294002, a specific inhibitor of PI3K, blocks phagolysosomal biogenesis (30, 32, 33). Bafilomycin A

markedly inhibited recruitment of cathepsin D to PVs in CD40-activated macrophages (86.7% ± 2.1% inhibition; $P = 0.001$) (Figure 6C). Bafilomycin A significantly inhibited toxoplasmacidal activity induced by CD40 stimulation (92.4% ± 3.4% inhibition; $P < 0.0001$) (Figure 6, D and E). In contrast, bafilomycin A did not affect the percentage of infection or the parasite load in control macrophages and IFN-γ/LPS–activated macrophages. The anti–*T. gondii* activity induced by IFN-γ/LPS was dependent on RNI since it was blocked by N^G-monomethyl-L-arginine (92% ± 4% inhibition; not shown) (23). Similar results were obtained with LY294002 (Supplemental Figure 2, C–E).

Next, we used genetic approaches to confirm that blocking of fusion ablates antimicrobial activity induced by CD40. These experiments were conducted using RAW 264.7 cells, which express a chimera that consists of the extracellular domain of human CD40 and the intracytoplasmic domain of mouse CD40 (hmCD40). Engagement of the chimera by human CD154 (hCD154) not only resulted in a strong anti–*T. gondii* activity (68.6% ± 1.7% reduction in parasite load) (29) but also induced vacuole/lysosome fusion. Incubation with hCD154 led to colocalization of cathepsin D and PVs in 40.5% ± 2.4% of hmCD40–RAW 264.7 cells (Figure 7B). We examined the effects of knockdown of PIK3C3 on vacuole/lysosome fusion and anti–*T. gondii* activity induced by CD40. Figure 7A shows that transfection of hmCD40–RAW 264.7 cells with antisense oligodeoxynucleotides (ODNs) against PIK3C3 diminished expression of this protein. Knockdown of PIK3C3 inhibited vacuole/lysosome fusion in *T. gondii*–infected hmCD40–RAW 264.7 cells stimulated with hCD154 (92.9% ± 2.0% inhibition; $P < 0.0001$) (Figure 7B). Importantly, knockdown of PIK3C3 markedly inhibited anti–*T. gondii* activity induced by CD40 stimulation (93.1% ± 5.5% inhibition; $P = 0.002$) (Figure 7C). In contrast, knockdown of PIK3C3 had no effect on parasite load in control hmCD40–RAW 264.7 cells and on the anti–*T. gondii* activity induced by IFN-γ/LPS.

Rab7 is pivotal for late endocytic trafficking and maintenance of a functional lysosome compartment (34, 35). Rab7 was excluded from *T. gondii*–containing vacuoles in control primary macrophages or hmCD40–RAW 264.7 cells (Figure 7D). In contrast, CD40 stimulation resulted in recruitment of Rab7 around PV in both types of macrophages (Figure 7D). Expression of Rab7 dominant-negative mutant impairs cargo degradation (36). Thus, we examined the effects of such a mutant on vacuole/lysosome fusion and anti–*T. gondii* activity induced by CD40 stimulation. Control or CD40-stimulated hmCD40–RAW 264.7 cells were transiently transfected with plasmids that encode Rab7 WT or the dominant-negative mutant Rab7(T22N). While cells transfected with Rab7 WT exhibited vacuole/lysosomal fusion, as assessed by colocalization of cathepsin D around PVs, transfection with Rab7(T22N) inhibited fusion (81.7% ± 5% inhibition; $P = 0.002$) (Figure 7E). Moreover, transfection with Rab7(T22N) impaired anti–*T. gondii* activity in response to CD40 stimulation (87.2% ± 6.0% inhibition; $P < 0.002$) but not IFN-γ/LPS (Figure 7F). Thus, multiple genetic and pharmacologic approaches demonstrate that vacuole/lysosome fusion mediates the antimicrobial activity induced by CD40 stimulation in macrophages.

CD40 triggers vacuole/lysosome fusion and antimicrobial activity through autophagy. Our studies indicate that CD40 signaling reroutes *T. gondii*–containing vacuoles to the late endosomal/lysosomal compartment. We hypothesized that vacuole/lysosome fusion induced by CD40 is mediated by autophagy, a process that can target organelles and cytoplasmic compartments to the lysosomes. We began by examining the expression of light chain 3 (LC3; Atg8), a highly specific marker of autophagosomes (37). Control and CD40-activated hmCD40–RAW 264.7 cells were transiently transfected with a plasmid that encodes LC3–enhanced GFP (LC3-EGFP). While control cells did not reveal colocalization of LC3 and PVs, CD40-activated hmCD40–RAW 264.7 cells exhibited increased expression of LC3 around these vacuoles (Figure 8A) ($P = 0.001$). Kinetic studies revealed that accumulation of LC3 around PVs preceded recruitment of LAMP-1 (Figure 8B).

Next, we determined whether autophagy mediates vacuole/lysosome fusion and antimicrobial activity induced by CD40. The autophagy protein Beclin 1 is essential for autophagosome formation (38). Thus, we ascertained whether knockdown of Beclin 1 impairs vacuole/lysosome fusion and antimicrobial activity induced by CD40. hmCD40–RAW 264.7 cells were transfected with either control siRNA or Beclin 1 siRNA. Figure 8C shows that transfection with Beclin 1 siRNA effectively reduced Beclin 1 protein expression. Next, we determined whether knockdown of Beclin 1 inhibits autophagosome formation. HmCD40–RAW 264.7 cells transfected with control or Beclin 1 siRNA were subsequently transfected with LC3-EGFP. Stimulation of autophagy by starvation resulted in redistribution of LC3 and formation of large $LC3^+$ structures (Figure 8C). In contrast, Beclin 1 siRNA impaired starvation-induced autophagosome formation. Importantly, knockdown of Beclin 1 markedly impaired colocalization of cathepsin D and PVs in CD40-activated hmCD40–RAW 264.7 cells (82.9% ± 6.3% inhibition; $P = 0.007$) (Figure 8D). Knockdown of Beclin 1 also inhibited anti–*T. gondii* activity induced by CD40 stimulation (90.2% ± 2.0% inhibition; $P = 0.007$) but not antimicrobial activity triggered by IFN-γ/LPS (Figure 8E). 3-Methyladenine (3-MA) is an inhibitor of autophagosome formation (39). 3-MA blocked vacuole/lysosome fusion (76.4% ± 1.9% inhibition; $P = 0.002$) and antimicrobial activity (82.4% ± 5.9% inhibition; $P = 0.002$) of CD40-activated primary human macrophages (Figure 8, F and G). Taken together, CD40 stimulation of macrophages triggers autophagy-dependent fusion between *T. gondii*–containing vacuoles and lysosomes, resulting in antimicrobial activity. To further confirm that autophagy can control the growth of *T. gondii*, macrophages were treated with rapamycin, an inducer of autophagy (40). RAW 264.7 cells transfected with LC3-EGFP and subsequently treated with rapamycin revealed colocalization of LC3 around PVs (Supplemental Figure 3A). Rapamycin treatment induced macrophage anti–*T. gondii* activity in RAW 264.7 cells that was blocked by transfection with Beclin 1 siRNA (88.4% ± 6.5% inhibition; $P < 0.0001$) (Supplemental Figure 3B). In addition, rapamycin induced anti–*T. gondii* activity in primary mouse macrophages that was significantly inhibited by treatment with 3-MA (79.5% ± 7.5% inhibition; $P = 0.003$) (Supplemental Figure 3C). Thus, autophagy leads to anti–*T. gondii* activity in macrophages.

Discussion

Understanding the regulation of effector mechanisms of pathogen elimination is pivotal for devising approaches to enhance host protection. A crucial question is whether CMI can alter the fate of an intracellular pathogen by inducing convergence between pathogen-containing vacuoles and lysosomes. We report 3 important findings that we believe represent a significant advance in

this area of research: (a) CMI can trigger killing of a pathogen within macrophages by inducing vacuole/lysosome fusion, and it does so through ligation of CD40, a molecule central to in vivo resistance against numerous pathogens; (b) Autophagy can be utilized by CMI as a mechanism of pathogen killing, a process that is controlled by CD40 engagement; (c) CD40 stimulation of macrophages changes the nonfusogenic nature of *T. gondii*–containing PVs, resulting in convergence with the late endosomal/lysosomal compartments. These findings provide new insight into fundamental aspects of host-pathogen interaction and mechanisms of host protection and uncover a mechanism by which CMI can alter the fate of an intracellular pathogen.

CD40-activated macrophages exhibit colocalization of Rab7, M6PR, LAMP-1, LAMP-2, CD63, and cathepsin D around PVs together with overlap between these vacuoles and LysoTracker Red; these findings are compatible with CD40-induced vacuole/lysosome fusion (5). Importantly, using multiple genetic and pharmacologic approaches, we demonstrate that vacuole/lysosome fusion mediates the microbicidal activity induced by CD40 in macrophages. Thus, CD40 is a novel regulator of vacuole/lysosome fusion in macrophages and triggers macrophage microbicidal activity through this mechanism.

The fate of *T. gondii* has been considered to be determined at the time of invasion (5, 6). PVs were deemed to remain nonfusogenic once they are formed (5, 6). By detecting dense granule secretion into the lumen of the vacuole — a key process during the formation of PV — we determined that CD40 stimulation resulted in fusogenicity of PVs. Moreover, engagement of CD40 by activated ($CD154^+$) $CD4^+$ T cells or anti-CD40 mAbs hours after formation of PVs resulted in vacuole/lysosome fusion. Thus, CMI can alter a key aspect of *T. gondii*–host cell interaction. *T. gondii* is an example of a pathogen that cannot survive within the lysosomal compartment. Hence, rerouting of the parasite to this site results in pathogen elimination.

We hypothesized that a switch in the fusogenic potential of PVs may be mediated by convergence of these vacuoles with the autophagic pathway since the latter process can direct to the lysosomal compartment organelles and cytosol that would otherwise not be targeted to lysosomes. Indeed, the autophagy marker LC3 colocalized with PVs in CD40-activated macrophages. Dissociation of LC3 from the autophagosome after its formation and enzymatic degradation of LC3 (41) likely explain why the percentage of PVs with detectable LC3 colocalization was lower than that of those that colocalized with late endosomal/lysosomal markers. Knockdown of Beclin 1 and treatment with 3-MA further implicated autophagy as a mechanism to overcome the fusion incompetence of PV. Lastly, bafilomycin A and LY294002, drugs known to inhibit degradation of contents within autolysosomes and autophagosome formation, respectively (42, 43), also inhibit vacuole/lysosome fusion. Taken together, our studies reveal that CD40 is a novel regulator of autophagy and utilizes this process to mediate killing of an intracellular pathogen in macrophages. These findings are important because, while studies thus far have reported that autophagy can result in pathogen degradation and it has been proposed that a rapid induction of autophagy may lead to control of *Legionella pneumophila* (44), it was unclear whether CMI restrains pathogens through induction of autophagy.

Multiple late endosomal/lysosomal markers colocalized with PV in CD40-activated macrophages. In contrast, we could not detect recruitment of early endosomal markers. These findings may be explained by convergence of autophagosomes with the endocytic pathway after the early endosome stage (45). Our studies on Rab7 and PIK3C3 are also relevant to the biology of autophagy. Rab7 and PIK3C3 not only control transport toward the lysosome in classical phagolysosome fusion (31, 46), but they are also central for autophagy. PIK3C3 is key for autophagosome formation (47, 48) while Rab7 is recruited to autophagosomes and controls their maturation, probably by regulating fusion with lysosomes (49, 50). Thus, the studies on manipulation of Rab7 and PIK3C3 not only reveal that vacuole/lysosome fusion mediates the antimicrobial activity induced by CD40, but they also indicate that these key players in autophagy were essential for vacuole/lysosome fusion induced by CD40.

Lysosomal hydrolytic enzymes, including cathepsins, are central for degradation of intracellular material. Our studies reveal that CD40 stimulation induces colocalization of cathepsin D with PVs. Moreover, studies using proteinase inhibitors indicate that pathogen eradication is dependent on the activity of these hydrolytic enzymes. Thus, in addition to delivering lysosomal enzymes to the vacuole, these findings suggest that CD40 stimulation also promotes activation of cathepsins and change of intravacuolar pH to that optimal for the function of these enzymes. These effects are in keeping with the central role of lysosomes in autophagy, in which autophagosomes acquire hydrolytic enzymes through convergence with the lysosomal compartment followed by digestion of the sequestered material.

While molecules involved in host protection have been well described, the mechanisms by which they lead to killing of a pathogen like *T. gondii* have remained elusive. In a model of mycobacterial infection, it was proposed that IFN-γ induces microbicidal activity by triggering phagosome maturation through autophagy (17). Our studies as well as those of others (11) revealed no evidence that IFN-γ triggers anti–*T. gondii* activity by inducing autophagy and vacuole/lysosome fusion. It was recently reported that IFN-γ induces toxoplasmacidal activity in mouse astrocytes by inducing disruption of PVs through a mechanism that requires the p47 GTPase IIGP1 (11). The fact that humans have only a single full-length p47GTPase that lacks IFN response elements and a truncated presumed pseudogene (51) would argue for the existence of other mechanisms of pathogen eradication. Indeed, not only is the toxoplasmacidal activity induced by CD40 independent of p47 GTPases (24), but this effector response as well as vacuole/lysosome fusion take place in both human and mouse macrophages.

The immune response against intracellular pathogens is multifaceted. While IFN-γ is central for resistance against these organisms, many lines of evidence indicate that there are additional mechanisms of host protection. In the case of *T. gondii*, patients with autosomal dominant mutation in IFN-γ receptor 1 (IFN-γR1) control *T. gondii* infection (52) despite the fact that this mutation removes the intracellular binding site for STAT1, a signaling molecule essential for control of *T. gondii* in mice (53). In addition, mice that lack T cells, CD154, or TNF-α die of toxoplasmosis despite elevated in vivo levels of IFN-γ (18, 54, 55). The CD40/CD154 pathway controls IFN-γ–independent mechanisms of resistance. Not only does CD40 stimulation in vitro induce a strong toxoplasmacidal activity in $CD40^+$ macrophages, but CD40 ligation in vivo induces killing of *T. gondii* by macrophages and reduces parasite load independently of IFN-γ and STAT1, a signaling molecule that controls RNI production and p47 GTPase activation (24).

In summary, our studies indicate that fundamental aspects of host-pathogen interaction can be modified by CD40 signaling. This work identifies CD40 as a pathway by which CMI alters the fate of an intracellular pathogen by controlling vacuole/lysosome fusion through autophagy. Thus, autophagy can act as a mechanism of pathogen eradication triggered by adaptive immunity. The fact that numerous pathogens survive by avoiding targeting to lysosomes raises the possibility that modulation of CD40 signaling and autophagy may be used as a therapeutic approach to eradicating pathogens.

Methods

Macrophages. Human monocyte–derived macrophages, mouse resident peritoneal macrophages, mouse bone marrow macrophages from either healthy volunteers or C57BL/6, BALB/c, or TNF-$\alpha^{-/-}$ mice, and hmCD40–RAW 264.7 cells were obtained as described (23, 25, 29). Macrophages were incubated with either a stimulatory anti-mouse CD40 mAb or hCD154 (gift from W. Fanslow, Amgen, Thousand Oaks, California, USA) for 24 and 48 hours prior to infection with *T. gondii*, respectively (29). CD40 engagement took place after infection in experiments that used CPSII KO *T. gondii*. In certain experiments, mouse macrophages were cultured with resting or activated $CD4^+$ T cells. These cells were obtained from uninfected BALB/c mice or IFN-$\gamma^{-/-}$ mice (BALB/c background) by incubation of spleen cells with anti-CD4–coated magnetic beads followed by culture with or without immobilized anti-CD3 plus anti-CD28 monoclonal antibodies. After 24 hours of incubation, $CD4^+$ T cells were added to macrophages 1 hour after infection with *T. gondii*. Animal studies were approved by the Institutional Animal Care and Use Committee of the University of Cincinnati.

Transgenic parasites. *T. gondii* RH parasites were maintained in human foreskin fibroblasts following standard procedures (56). Parasites expressing cytoplasmic YFP have been described (57, 58). Parasites expressing cytoplasmic DsRed (RFP) were generated by transfection with *ptub*P30RFP/*sag*CAT plasmid, kindly provided by F. Dzierszinski (University of Pennsylvania, Philadelphia, Pennsylvania, USA) (58). Transgenic CPSII KO *T. gondii* that express cytoplasmic YFP (28, 58) were a kind gift from D. Roos (University of Pennsylvania, Philadelphia, Pennsylvania, USA). Parasites expressing secreted DsRed (secRFP) were transfected with plasmid *ptub*-P30RFP/*sag*CAT (59). All parasite lines were selected for stable expression of the transgene under drug selection and cloned by limiting dilution.

T. gondii infection. Macrophages were challenged for 5 to 10 minutes with transgenic *T. gondii* that express cytoplasmic YFP, cytoplasmic RFP, or secRFP or with transgenic CPSII KO *T. gondii* that express cytoplasmic YFP. Monolayers were washed to remove extracellular parasites and used for immunofluorescence analysis. Monolayers were also infected with nonfluorescent RH *T. gondii* and examined by light microscopy (23). Changes in the percentage of infected cells were not due to differences in cell detachment during processing of samples (23). In addition, cell densities as determined with an eyepiece grid were similar in all experimental groups (23). In certain experiments, monolayers were treated with: Bafilomycin A1 (25 nM; Sigma-Aldrich) beginning 1 hour prior to infection. LY294002 (20 nM; Sigma-Aldrich), pepstatin (50 μM; Sigma-Aldrich), leupeptin (2 mg/ml; Calbiochem; EMD Biosciences), or 3-MA (10 mM; Sigma-Aldrich) were added to monolayers 1 hour after infection. Rapamycin (1 μM; Calbiochem; EMD Biosciences) was added to macrophages 2 hours after infection with *T. gondii*. Effects of experimental conditions were confirmed when blinded samples were scored.

Transfections. HmCD40–RAW 264.7 cells preincubated with or without hCD154 for 24 hours were transiently transfected with plasmids encoding EGFP-Rab7 WT, EGFP-Rab7(T22N) (gift from C. Roy, Yale University, New Haven, Connecticut, USA), or LC3-EGFP (gift from T. Yoshimori, National Institute for Basic Biology, Okazaki, Japan) using an Amaxa Nucleofector. Cells were cultured with or without hCD154 for an additional 18 hours prior to infection with *T. gondii*.

Knockdown of Beclin 1 was performed by transfecting hmCD40–RAW 264.7 cells with either control or a previously described Beclin 1 siRNA (60) (Dharmacon), using an Amaxa Nucleofector. Knockdown of PIK3C3 was performed using phosphorothioate-modified ODN (Integrated DNA Technologies). The antisense ODN had the following sequence: 5′-CCA-CAGGCCCTTCAAATG -3′. hmCD40–RAW 264.7 cells were incubated with either sense or antisense ODN (25 μM) in the presence of Lipofectamine 2000 (Invitrogen). Cells were subsequently incubated for 48 hours in medium with or without hCD154, then infected with *T. gondii*.

Immunofluorescence and confocal microscopy. Macrophages were fixed with 4% paraformaldehyde. Cells were permeabilized either with 0.1% Triton X-100 in PBS or ice-cold methanol followed by incubation in blocking buffer. Macrophages challenged with *T. gondii* secRFP were fixed and permeabilized with methanol without prior exposure to paraformaldehyde. Monolayers were incubated with the following antibodies overnight at 4°C: mouse anti-human LAMP-1, rat anti-mouse LAMP-1, rat anti-mouse LAMP-2 (all from Developmental Studies Hybridoma Bank), mouse anti-human CD63, anti-human cathepsin D (both from Chemicon International), goat anti-mouse Cathepsin D (R&D Systems), chicken anti-mouse M6PR (Chemicon International), mouse anti-Rab5 and anti-EEA1 (both from BD Biosciences), goat anti-Rab7 (Santa Cruz Biotechnology Inc.). Monolayers were washed with PBS plus 1% BSA, then incubated for 1 hour at room temperature with Alexa 568–, Texas red–, Cy2-, or Cy5-conjugated secondary antibodies (Alexa 568, Invitrogen; Texas red, Cy2, and Cy5, Jackson ImmunoResearch Laboratories Inc.). Antibodies did not cross-react with opsonized or nonopsonized *T. gondii*. Slides were mounted using Fluormount G (SouthernBiotech). Specificity of staining was determined by incubating monolayers with control primary antibody plus secondary antibody or with secondary antibody alone. Monolayers were analyzed using a LSM 510 laser scanning confocal microscope (Zeiss) or a Zeiss Axioplan epifluorescence microscope equipped with an ORCA-ER camera (Opelco). For LysoTracker colocalization studies, macrophages were preloaded with LysoTracker Red DND-99 (1:20,000; Invitrogen) for 2 hours prior to infection. LysoTracker Red was re-added after removal of *T. gondii*. Colocalization with endosomal/lysosomal markers was deemed to have taken place if there was a continuous accumulation of staining around the vacuole (ring) (5) or if staining was distributed within PVs covering the parasite (LysoTracker Red). Macrophages that phagocytosed opsonized *T. gondii* were used as positive controls. To this end, tachyzoites were incubated with either dye-test positive (1:30,000) human serum or anti-SAG1 monoclonal antibody (DG52; gift from J. Boothroyd, Stanford University, Stanford, California, USA) before addition to human or mouse macrophages, respectively. Heat-killed tachyzoites (10 minutes incubation at 56°C) were also used as controls. Effects of experimental conditions were confirmed when "blinded" samples were scored.

To detect membrane CD40, monolayers were incubated with blocking buffer, then with biotinylated anti-CD40 monoclonal antibody (eBioscience) or hamster IgM for 30 minutes at 4°C (23). After washing with blocking buffer, monolayers were incubated with streptavidin–Alexa 647 (Invitrogen) for 30 minutes on ice. Slides were washed, fixed with 4% paraformaldehyde, and processed for staining of endosomal/lysosomal markers as described above.

To determine the percentages of cell-associated tachyzoites that were intracellular, monolayers of macrophages infected with *T. gondii*–YFP were fixed with paraformaldehyde, then incubated with an anti-SAG1

antibody without prior permeabilization. Monolayers were stained with Alexa 568–conjugated secondary antibody. Intracellular tachyzoites displayed only green fluorescence while extracellular ones exhibited both green and red fluorescence.

Immunoblot. hmCD40–RAW 264.7 cells transfected with sense or antisense PIK3C3 ODN or with control or Beclin 1 siRNA were lysed 48 hours and 96 hours after transfection, respectively, and proteins were resolved on 10% SDS-PAGE. Antibodies used were directed against hVps34 (Zymed; Invitrogen), Beclin 1 (BD Biosciences), or actin (Santa Cruz Biotechnology Inc.).

Statistics. Statistical significance was assessed by 2-tailed Student's *t* test and ANOVA. Values less than 0.05 were considered statistically significant.

Acknowledgments

We are grateful to David Roos and Beth Levine for helpful suggestions. We thank Cecilia Subauste and Christopher Hunter for review of this manuscript. We thank David Roos and Florence Dzierszinski for providing transgenic *T. gondii* and Tamotsu Yoshimori, John Boothroyd, William Fanslow, and Craig Roy for providing reagents. This work was supported by NIH grant AI48406 (to C.S. Subauste) and the American Heart Association, Ohio Valley Affiliate (to C.S. Subauste). B. Striepen and M.-J. Gubbels are supported by grants from the NIH and the American Heart Association, respectively.

Received for publication April 11, 2006, and accepted in revised form June 27, 2006.

Address correspondence to: Carlos S. Subauste, Departments of Ophthalmology and Medicine, Case Western Reserve University School of Medicine, 11100 Euclid Avenue, Cleveland, Ohio 44106, USA. Phone: (216) 844-8590; Fax: (216) 844-7117; E-mail: carlos.subauste@case.edu.

Marc-Jan Gubbels' present address is: Department of Biology, Boston College, Chestnut Hill, Massachusetts, USA.

Carlos S. Subauste's present address is: Departments of Ophthalmology and Medicine, Case Western Reserve University School of Medicine, Cleveland, Ohio, USA.

1. Sinai, A.P., and Joiner, K.A. 1997. Safe haven: the cell biology of nonfusogenic pathogen vacuoles. *Ann. Rev. Microbiol.* **51**:415–462.
2. Meresse, S., et al. 1999. Controlling the maturation of pathogen-containing vacuoles: a matter of life or death. *Nat. Cell Biol.* **1**:E183–E188.
3. Amer, A.O., and Swanson, M.S. 2002. A phagosome of one's own: a microbial guide to life in the macrophage. *Curr. Opin. Microbiol.* **5**:56–61.
4. Coppens, I., et al. 2006. *Toxoplasma gondii* sequesters lysosomes from mammalian hosts in the vacuolar space. *Cell.* **125**:261–274.
5. Mordue, D.G., and Sibley, L.D. 1997. Intracellular fate of vacuoles containing *Toxoplasma gondii* is determined at the time of formation and depends on the mechanisms of entry. *J. Immunol.* **159**:4452–4459.
6. Joiner, K.A., Fuhrman, S.A., Mietinnen, H., Kasper, L.H., and Mellman, I. 1990. *Toxoplasma gondii*: fusion competence of parasitophorous vacuoles in Fc receptor transfected fibroblasts. *Science.* **249**:641–646.
7. Blander, J.M., and Medzhitov, R. 2004. Regulation of phagosome maturation by signals from toll-like receptors. *Science.* **304**:1014–1018.
8. Yates, R.M., and Russell, D.G. 2005. Phagosome maturation proceeds independently of stimulation of toll-like receptors 2 and 4. *Immunity.* **23**:409–417.
9. Schaible, U.E., Sturgill-Koszycki, S., Schlesinger, P.H., and Russell, D.G. 1998. Cytokine activation leads to acidification and increases maturation of *Mycobacterium avium*-containing phagosomes in murine macrophages. *J. Immunol.* **160**:1290–1296.
10. MacMicking, J.D., Taylor, G.A., and McKinney, J.D. 2003. Immune control of tuberculosis by IFN-γ-inducible LRG-47. *Science.* **302**:654–659.
11. Martens, S., et al. 2005. Disruption of *Toxoplasma gondii* parasitophorous vacuoles by the mouse p47-resistance GTPases. *PLoS Pathog.* **1**:187–201.
12. Levine, B., and Klionsky, D.J. 2004. Development by self-digestion: molecular mechanisms and biological functions of autophagy. *Dev. Cell.* **6**:463–477.
13. Mizushima, N., Ohsumi, Y., and Yoshimori, T. 2002. Autophagosome formation in mammalian cells. *Cell Struct. Funct.* **27**:421–429.
14. Dunn, W.A.J. 1994. Autophagy and related mechanisms of lysosome-mediated protein degradation. *Trends Cell Biol.* **110**:1923–1933.
15. Nakagawa, I., et al. 2004. Autophagy defends cells against invading group A *Streptococcus*. *Science.* **306**:1037–1040.
16. Ogawa, M., et al. 2004. Escape of intracellular *Shigella* from autophagy. *Science.* **307**:727–731.
17. Gutierrez, M.G., et al. 2004. Autophagy is defense mechanism inhibiting BCG and *Mycobacterium tuberculosis* survival in infected macrophages. *Cell.* **119**:753–766.
18. Reichmann, G., et al. 2000. The CD40/CD40 ligand interaction is required for resistance to toxoplasmic encephalitis. *Infect. Immun.* **68**:1312–1318.
19. Soong, L., et al. 1996. Disruption of CD40-CD40 ligand interactions results in an enhanced susceptibility to *Leishmania amazoniensis* infection. *Immunity.* **4**:263–273.
20. Kamanaka, M., et al. 1996. Protective role of CD40 in *Leishmania major* infection at two distinct phases of cell-mediated immunity. *Immunity.* **4**:275–281.
21. Hayashi, T., Rao, S.P., Meylan, P.R., Kornbluth, R.S., and Catanzaro, A. 1999. Role of CD40 ligand in *Mycobacterium avium* infection. *Infect. Immun.* **67**:3558–3565.
22. Netea, M.G., van der Meer, J.W.M., Verschueren, I., and Kullberg, B.J. 2002. CD40/CD40 ligand interactions in the host defense against disseminated *Candida albicans* infection: the role of macrophage-derived nitric oxide. *Eur. J. Immunol.* **32**:1455–1463.
23. Andrade, R.M., Portillo, J.-A.C., Wessendarp, M., and Subauste, C.S. 2005. CD40 signaling in macrophages induces activity against an intracellular pathogen independently of γ interferon and reactive nitrogen intermediates. *Infect. Immun.* **73**:3115–3123.
24. Subauste, C.S., and Wessendarp, M. 2006. CD40 restrains the in vivo growth of *Toxoplasma gondii* independently of gamma interferon. *Infect. Immun.* **74**:1573–1579.
25. Andrade, R.M., Wessendarp, M., and Subauste, C.S. 2003. CD154 activates macrophage anti-microbial activity in the absence of IFN-γ through a TNF-α-dependent mechanism. *J. Immunol.* **171**:6750–6756.
26. Carruthers, V.B., and Sibley, D. 1997. Sequential protein secretion from three distinct organelles of *Toxoplasma gondii* accompanies invasion of human fibroblasts. *Eur. J. Cell Biol.* **73**:114–123.
27. Striepen, B., He, C.Y., Matrajt, M., Soldati, D., and Roos, D.S. 1998. Expression, selection, and organellar targeting of the green fluorescent protein in *Toxoplasma gondii*. *Mol. Biochem. Parasitol.* **92**:325–338.
28. Fox, B.A., and Bzik, D.J. 2002. De novo pyrimidine biosynthesis is required for virulence of *Toxoplasma gondii*. *Nature.* **415**:926–929.
29. Andrade, R.M., et al. 2005. TRAF6 signaling downstream of CD40 primes macrophages to acquire anti-microbial activity in response to TNF-α. *J. Immunol.* **175**:6014–6021.
30. van Weert, A.W., Dunn, K.W., Gueze, H.J., Maxfield, F.R., and Stoorvogel, W. 1995. Transport from late endosomes to lysosomes, but not sorting of integral membrane proteins in endosomes, depends on the vacuolar proton pump. *J. Cell Biol.* **130**:821–834.
31. Stein, M.P., Feng, Y., Cooper, K.L., Welford, A.M., and Wandinger-Ness, A. 2003. Human VPS34 and p150 are Rab7 interacting partners. *Traffic.* **4**:754–771.
32. Yates, R.M., Hermetter, A., and Russell, D.G. 2005. The kinetics of phagosome maturation as a function of phagosome/lysosome fusion and acquisition of hydrolytic activity. *Traffic.* **6**:413–420.
33. Fratti, R.A., Backer, J.M., Gruenberg, J., Corvera, S., and Deretic, V. 2001. Role of phosphatidylinositol 3-kinase and Rab5 effectors in phagosomal biogenesis and mycobacterial phagosome arrest. *J. Cell Biol.* **154**:631–644.
34. Feng, Y., Press, B., and Wandinger-Ness, A. 1995. Rab 7: an important regulator of late endocytic membrane traffic. *J. Cell Biol.* **131**:1435–1452.
35. Bucci, C., Thomsen, P., Nicoziani, P., McCarthy, J., and van Deurs, B. 2000. Rab7: a key to lysosome biogenesis. *Mol. Biol. Cell.* **11**:467–480.
36. Vitelli, R., et al. 1997. Role of small GTPase Rab7 in the late endocytic pathway. *J. Biol. Chem.* **272**:4391–4397.
37. Kabeya, Y., et al. 2000. LC3, a mammalian homologue of yeast Apg8p, is localized in autophagosome membranes after processing. *EMBO J.* **19**:5720–5728.
38. Kihara, A., Kabeya, Y., Ohsumi, Y., and Yoshimori, T. 2001. Beclin-phosphatidylinositol 3-kinase complex functions at the *trans*-Golgi network. *EMBO J.* **21**:330–335.
39. Seglen, P.O., and Gordon, P.B. 1982. 3-Methyladenine: specific inhibitor of autophagic/lysosomal protein degradation in isolated rat hepatocytes. *Proc. Natl. Acad. Sci. U. S. A.* **79**:1889–1892.
40. Noda, T., and Ohsumi, Y. 1998. Tor, a phosphatidylinositol kinase homologue, controls autophagy in yeasts. *J. Biol. Chem.* **273**:3963–3966.
41. Reggiori, F., and Klionsky, D.J. 2005. Autophagosomes: biogenesis from scratch? *Curr. Opin. Cell Biol.* **17**:1–8.
42. Mousavi, S.A., et al. 2001. Effects of inhibitors of the vacuolar proton pump on hepatic heterophagy and autophagy. *Biochim. Biophys. Acta.* **1510**:243–257.
43. Blommaart, E.F., Krause, U., Schellens, J.P., Vreeling-Sindelarova, H., and Meijer, A.J. 1997. The

phosphatidylinositol 3-kinase inhibitors wortmannin and LY294002 inhibit autophagy in isolated rat hepatocytes. *Eur. J. Biochem.* **243**:240–246.
44. Amer, A.O., and Swanson, M.S. 2005. Autophagy is an immediate macrophage response to *Legionella pneumophila*. *Cell. Microbiol.* **7**:765–778.
45. Tooze, J., et al. 1990. In exocrine pancreas, the basolateral endocytic pathway converges with the autophagic pathway immediately after the early endosome. *J. Cell Biol.* **111**:329–345.
46. Via, L.E., et al. 1997. Arrest of mycobacterial phagosome maturation is caused by a block in vesicle fusion between stages controlled by rab5 and rab7. *J. Biol. Chem.* **272**:13326–13331.
47. Kihara, A., Noda, T., Ishihara, N., and Ohsumi, Y. 2001. Two distinct Vps34 phosphatidylinositol 3-kinase complexes function in autophagy and carboxypeptidase Y sorting in *Saccharomyces cerevisiae*. *J. Cell Biol.* **152**:519–530.
48. Petiot, A., Ogier-Denis, E., Blommaart, E.F., Meijer, A.J., and Codogno, P. 2000. Distinct classes of phosphatidylinositol 3′-kinases are involved in signaling pathways that control macroautophagy in HT-29 cells. *J. Biol. Chem.* **275**:992–998.
49. Gutierrez, M.G., Munafo, D.B., Beron, W., and Colombo, M.C. 2004. Rab7 is required for the normal progression of the autophagic pathway in mammalian cells. *J. Cell Sci.* **117**:2687–2697.
50. Jager, S., et al. 2004. Role for Rab7 in maturation of late autophagic vacuoles. *J. Cell Sci.* **177**:4837–4848.
51. Bekpen, C., et al. 2005. The interferon-inducible p47 (IRG) GTPases in vertebrates: loss of the cell autonomous resistance mechanism in the human lineage. *Genome Biol.* **6**:R92.
52. Janssen, R., et al. 2002. Divergent role for TNF-α in IFN-γ-induced killing of *Toxoplasma gondii* and *Salmonella typhimurium* contributes to selective susceptibility of patients with partial IFN-γ receptor 1 deficiency. *J. Immunol.* **169**:3900–3907.
53. Lieberman, L.A., Banica, M., Reiner, S.L., and Hunter, C.A. 2004. STAT1 plays a critical role in the regulation of antimicrobial effector mechanisms, but not in the development of Th1-type responses during toxoplasmosis. *J. Immunol.* **172**:457–463.
54. Hunter, C.A., Subauste, C.S., van Cleave, V.H., and Remington, J.S. 1994. Production of gamma interferon by natural killer cells from *Toxoplasma gondii*-infected SCID mice: regulation by interleukin-10, interleukin-12 and tumor necrosis factor alpha. *Infect. Immun.* **62**:2818–2824.
55. Yap, G.S., Scharton-Kersten, T., Charest, H., and Sher, A. 1998. Decreased resistance of TNF receptor p55- and p75-deficient mice to chronic toxoplasmosis despite normal activation of inducible nitric oxide synthase in vivo. *J. Immunol.* **160**:1340–1345.
56. Roos, D.S., Donald, R.G., Morrissette, N.S., and Moulton, A.L. 1994. Molecular tools for genetic dissection of the protozoan parasite *Toxoplasma gondii*. *Methods Cell Biol.* **45**:27–63.
57. Gubbels, M.J., Li, C., and Striepen, B. 2003. High-throughput growth assay for *Toxoplasma gondii* using yellow fluorescent protein. *Antimicrob. Agents Chemother.* **47**:309–316.
58. McKee, A.S., Dzierszinski, F., Boes, M., Roos, D.S., and Pearce, E.J. 2004. Functional inactivation of immature dendritic cells by the intracellular parasite *Toxoplasma gondii*. *J. Immunol.* **173**:2632–2640.
59. Gubbels, M.J., Striepen, B., Shastri, N., Turkoz, M., and Robey, E.A. 2005. Class I major histocompatibility complex presentation of antigens that escape from the parasitophorous vacuole of *Toxoplasma gondii*. *Infect. Immun.* **73**:703–711.
60. Yu, L., et al. 2004. Regulation of an *ATG7-beclin 1* program of autophagic cell death by caspase-8. *Science.* **304**:1500–1502.